Asian Journal of Chemistry; Vol. 36, No. 5 (2024), 1045-1050

ASIAN JOURNAL OF CHEMISTRY

https://doi.org/10.14233/ajchem.2024.31256

# *Rivea hypocrateriformis* Plant Extract Mediated Synthesis of ZnO Nanoparticles: Characterization, Antioxidant and Anticancer Activities

M. BALAJI, P. RAJESH*, V. VELMANI, G.T. PARETHE and S. KAVICA

PG & Research Department of Chemistry, Government Arts College (Autonomous), Coimbatore-641018, India

*Corresponding author: E-mail: gacchemistryrajesh@gmail.com

*Received*: 16 January 2024; *Accepted*: 28 February 2024; *Published online*: 30 April 2024; AJC-21607

Nanomedicine has emerged as a promising approach for cancer diagnosis and treatment. This study explores the green synthesis of zinc oxide nanoparticles using *Rivea hypocrateriformis* extract. The synthesized ZnO nanoparticles were characterized through UV-vis, FT-IR, zeta potential, XRD, SEM with EDS and TEM analyses. These nanoparticles were also evaluated for their impact on A549 cell lines. The UV visible spectroscopy identified absorbance peaks, while FT-IR analysis detected various functional groups. SEM and XRD images confirmed the partial crystal spherical form and crystal nature. The cytotoxicity assessments revealed an enhanced cytotoxic effect, marking a significant step toward synthesizing ZnONPs as potential anticancer agents. This research suggests the potential of these nanoparticles as chemo-preventive agents in future cancer treatments, in addition to their strong antioxidant properties.

**Keywords: Green synthesis, Zinc oxide nanoparticles, *Rivea hypocrateriformis* extract, Antioxidant, Anticancer.**

## INTRODUCTION

Smoking, hormonal imbalances, virus infections and genetic factors are the main causes of lung cancer, which affects both men and women and is the most common type of cancer in developed countries. There are two main varieties of lung cancer, small cell (SCLCs) and non-small cell (NSCLCs) [1,2]. Despite the availability of conventional treatments such as surgery, chemotherapy and radiotherapy, patients often endure severe side effects and stress. Researchers are increasingly turning to nanomedicine as an alternative therapeutic approach for cancer diagnosis and treatment. World Health Organization (WHO) reports that approximately 75-80% of the global population still relies on traditional medical practices for their healthcare needs [3].

In the ongoing investigation, the plant under scrutiny has been subjected to a comprehensive evaluation, focusing on its potential cytotoxicity, antiproliferative properties and antimitotic effects on cancerous cell lines [4]. This study is emblematic of a broader trend in scientific research, where there is a growing interest in adopting environmentally friend methodologies that prevent the use of harmful chemicals and their associated byproducts [5].

The interest in investigating the potential of zinc oxide (ZnO) has significantly increased and remains a strong motivating factor in the research. ZnO appeal lies in its promising potential for applications in optoelectronics, owing to its wide direct band gap (approximately 3.4 eV), n-type semi conductivity, high reactivity in chemical reactions with catalysts, cost-effectiveness and its status as a non-toxic and luminous material [6]. Researchers have increasingly turned their attention to manipulating the morphologies and size distribution of ZnO nanoparticles. They have been actively involved in both the synthesis of new ZnO nanoparticles and the modification of existing ones.

The climbing shrub *Rivea hypocrateriformis* is native to India and is well-known for its many medicinal uses, such as its ability to treat diabetes, piles, burns, problems during pregnancy, implantation, depression, anxiety, cancer, anesthesia and liver protection. The plant is rich in phytochemical constituents like amino acids, lupeol and gallic acid, which may hold promise for cytotoxicity applications. During the synthesis of metallic nanoparticles, the plant extracts which are rich in compounds like polyphenols, amino acids, carboxylic groups, *etc*. and can be used for both stabilizing and reducing in nanoparticle synthesis [3]. Literature review reveals a lack of prior research on *R. hypocrateriformis* based ZnO nanomaterials. This intriguing gap in knowledge has motivated to explore the synthesis of

ZnO nanomaterials derived from *R. hypocrateriformis* and assess their cytotoxic potential.

## EXPERIMENTAL

Merck grade zinc sulphate heptahydrate ($ZnSO_4 \cdot 7H_2O$), sodium hydroxide and ethanol were purchased. The plant was collected from the local garden located at Rasipuram city of India (11.4615º N, 78.1855º E).

**Plant extract:** The *Rivea hypocrateriformis* plant were thoroughly washed with tap water followed by distilled water and dried under air room temperature for 15 days. Then these dried plants were blended to a finely powder. The powdered plant (50 g) were placed in a Soxhlet apparatus containing 100 mL ethanol and the process was allowed to run around 12 h.

**Synthesis of zinc oxide (ZnO) nanoparticles:** The zinc oxide nanoparticles were synthesized by precipitation method in which various promenient functional groups present in plant act as good stabilizing agent and result in the formation of nanoparticles. In short, 60 mL of aqueous plant extract was mixed with 100 mL of 0.1 M aqueous solution of $ZnSO_4 \cdot 7H_2O$ in a beaker and then stirred the solution using a magnetic stirrer for 1 h followed by the addition of NaOH solution dropwise until the optimum pH attained. The resultant extract solution was centrifuged 10000 rpm for 15 min, the supernatant was discarded and the pellet containing precipitate of ZnO nanoparticles was collected and washed with ethanol to remove impurities and then dried in an oven at 80 ºC.

**Characterization:** The absorbance spectra of the ZnO nanoparticles were studied using UV visible spectrophotometer (Hitachi, U-3010). The surface factualization of plant extract on the surface of zinc oxide nanoparticles were studied by FTIR (Perkin-Elmer 65) in the wavenumber range of 4000 to 400 $cm^{-1}$. The crystalline nature and phase identification were studied by XRD technique using Empyrean Malvern Panalytical instrument with Cu$K\alpha$ ($\lambda$ = 1.54 Å) radiation as X-ray source at a 10-80º diffraction angle. The surface morphology of the prepared nanoparticle were analyzed by scanning electron microscopic technique using Carl Zeiss (USA) model–Sigma with Gemini column instrument. The EDS analysis was also performed to estimate the elemental composition of the biosynthesized ZnO nanoparticles. Transmission electron microscope (TEM) was used to analyze the morphological and structural characteristics of the biosynthesized ZnO nanostructures using JEOL-JEM 2100 TEM instrument operated at a 200 kV accelerating voltage.

**Antioxidant activity:** The antioxidant activity of sample zinc oxide nanoparticles was examined by stable DPPH free radical activity. The 0.1 mM, 100 µL of DPPH solution was added to 300 µL of biosynthesized ZnO nanoparticles at different concentration (500, 250, 100, 50 and 10 µg/mL). Then 96% (2.7 mL) of methanol was added in the mixture, shaked vigorously and allowed to stand for 5 min. The absorbance was measured spectrophotometrically at 517 nm. The experiments were performed in triplicate. The radical activity of biosynthesized ZnO nanoparticles was expressed as percentage of inhibition using the following eqn. 1:

$$\text{Inhibition of DPPH activity (\%)} = \frac{A - B}{A} \times 100$$

where A and B are the absorbance values of blank and sample, respectively. A curve of concentration *versus* percentage inhibition was plotted and concentration required for 50% inhibition was determined.

$$\text{DPPH scavenging effect (\%)} = \frac{A_{control} - A_{reaction\ mixture}}{A_{control}} \times 100$$

**Anticancer activity of ZnO nanoparticle**

**Cell culture:** A549 (human lung carcinoma cells) purchased from NCCS, Pune, India were cultured in liquid medium (DMEM) supplemented 10% fetal bovine serum (FBS), 100 µg/mL penicillin and 100 µg/mL streptomycin and maintained under an atmosphere of 5% $CO_2$ at 37 ºC.

**MTT assay:** The biosynthesized ZnO nanoparticles was tested for *in vitro* cytotoxicity using the A549 cells by MTT assay. Briefly, the cultured A549 cells were harvested and pooled in a 15 mL tube. Then, the cells were plated at a density of $1 \times 10^5$ cells/mL cells/well (200 µL) into the 96-well tissue culture plate in DMEM medium containing 10 % FBS and 1% antibiotic solution for 24-48 h at 37 ºC. The wells were washed with sterile phosphate buffered saline (PBS) solution and treated with different concentrations of the ZnO nanoparticles in a serum-free DMEM medium. Each sample was replicated three times and the cells were incubated at 37 ºC in a humidified 5% $CO_2$ incubator for 24 h. After incubation, MTT (10 µL of 5 mg/mL) was added to each well and the cells were incubated for another 2-4 h until purple precipitate were clearly visible under an inverted microscope. Finally, the medium combined with MTT (220 µL) was aspirated off the wells and washed with 1X PBS (200 µL). Furthermore, to dissolve formazan crystals, DMSO (100 µL) was added and the plate was shaken for 5 min. The absorbance for each well was measured at 570 nm using a microplate reader (Thermo-Fisher Scientific, USA) and the percentage cell viability and $IC_{50}$ value were calculated using Graph Pad Prism 6.0 software (USA).

## RESULTS AND DISCUSSION

**UV-visible studies:** A prominent peak at 350 nm (Fig. 1a) confirmed the successful ZnO nanoparticles formation. The ZnO intrinsic band-gap absorption causes electron transfers from the valence to the conduction band [7]. With decreasing nanoparticle size, the absorption edge gradually advances to a lower wavelength or higher energy as shown by plant-mediated ZnO with precursor zinc sulphate at 287 nm (Fig. 1b) [8].

**FT-IR studies:** The FTIR analysis of *R. hypocrateriformis* extract was analyzed to determine the functional groups present and their role in the synthesis of ZnO nanoparticles. The FT-IR spectra of the plant extract (Fig. 2a) and the biosynthesized ZnO NPs (Fig. 2b) are shown. The intense and broad peak at 3594 $cm^{-1}$ is associated to H-bond hydroxyl group (–OH) stretching vibrational of phenol or alcoholic group [9], whereas the peak at 2997 $cm^{-1}$ is due to the -OH stretching carboxylic group. The peak at 2322 $cm^{-1}$ arised due to presnce of O=C=O

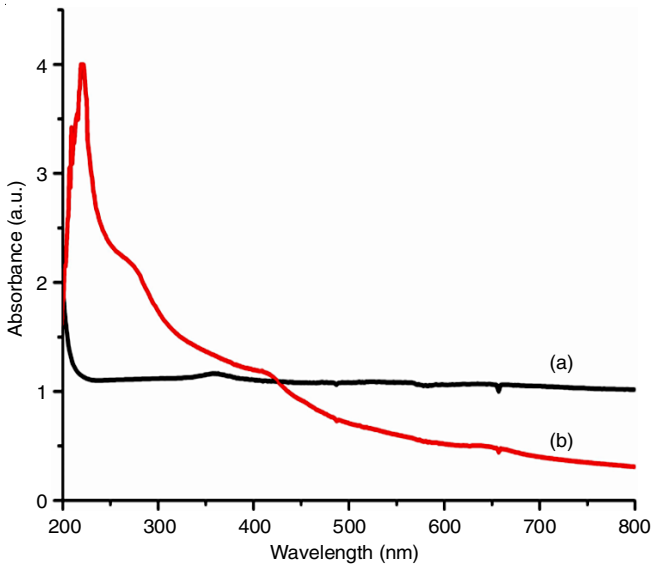


Fig. 1. UV spectrum (a) ZnO and (b) RH-ZnO NPs

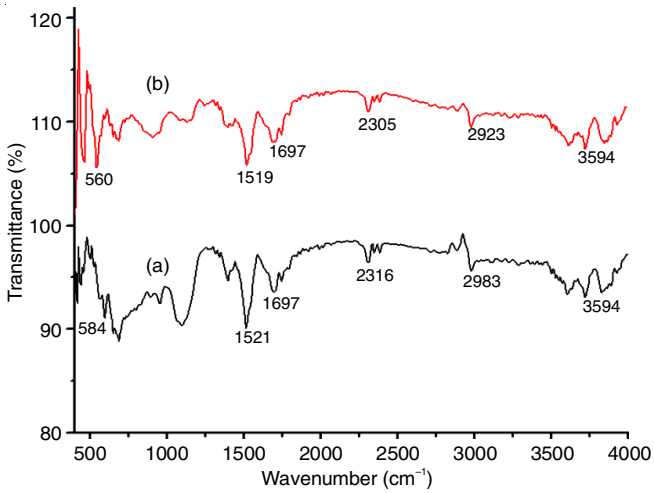


Fig. 2. FT-IR spectra (a) ZnO NPs and (b) RH-ZnO NPs

carbon dioxide, while the peaks at 1723 $cm^{-1}$ and 1697 $cm^{-1}$ are attributed to the C=O stretching aldehydic group. The peak at lower wavelength 1541 $cm^{-1}$ is due to the stretching $NO_2$ compounds and a peak at 1132 $cm^{-1}$ is associated to C-O tertiary alcohol group. A stretching vibration peak at 560 $cm^{-1}$ for Zn-O is also observed [10].

**XRD studies:** The X-ray diffraction pattern was adopted to study the structural properties of the prepared sample. The results were compared to the JCPDS Data and the peaks were identified along the planes (100), (002), (101), (102), (110) and (103) and in 2θ 31.73º, 34.43º, 36.27º, 47.70º, 56.6º and 62.81º as shown in Fig. 3, indicating that biosynthesized ZnO nanoparticles are crystalline in nature [11]. The XRD diffraction patterns revealed the hexagonal wurtzite structure of the nanoparticles, which were further confirmed by the JCPDS card no. 008, 82-1042 & 50,664 [12]. The particle sizes of the plant mediated ZnO nanoparticles were calculated using Debye-Scherrer's equation:

$$d = \frac{k\lambda}{\beta_{hkl}\cos\theta_{hkl}}$$

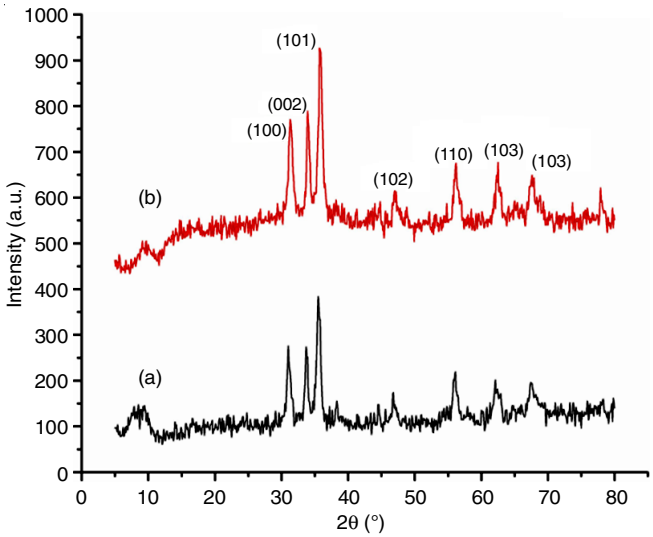


Fig. 3. XRD pattern (a) ZnO NPs and (b) RH-ZnO NPs

where d is the crystallite size of synthesized ZnO nanoparticles; k is Scherrer's constant (0.9); λ is the X-ray wavelength of radiation (1.5406 Å); $\beta_{hkl}$ is the full-width at half maximum (FWHM) at (*hkl*) peak in radian and $\theta_{hkl}$ is the diffraction angle.

**Zeta potential:** The biosynthesized ZnO nanoparticles exhibit good stability because of the repulsion between the particles, which was ensured by the negative sign of the zeta potential value [3]. The observed zeta potential value of the synthesized nanoparticles was found to be -16.128 mV (Fig. 4).

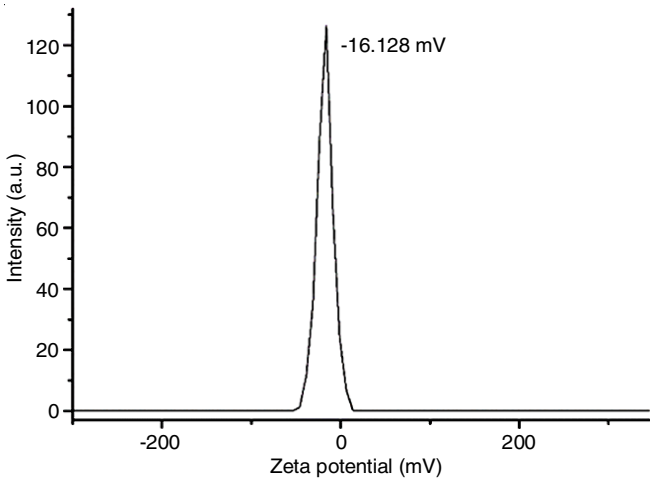


Fig. 4. Zeta potential of *R. hypocrateriformis* mediated ZnO nanoparticles

**SEM and EDS studies:** The SEM images were obtained at different levels of magnification indicated the flower-shaped RH-ZnO nanomaterial (Fig. 5). The development of evenly distributed RH-ZnO nanoflowers is clearly observed at lower magnifications. Formation of ZnO nanoparticles is confirmed by the chemical compositions analyzed by EDS analysis. As shown in Fig. 6, the synthesized ZnO nanoparticles contain zinc and oxygen as major elements.

**TEM studies:** TEM images illustrating that the RH-ZnO NPs, which resembled a flower, consisted of several leaf-shaped petals, with a distinct arrangement of hexagonal ZnO nanorods in each one (Fig. 7).

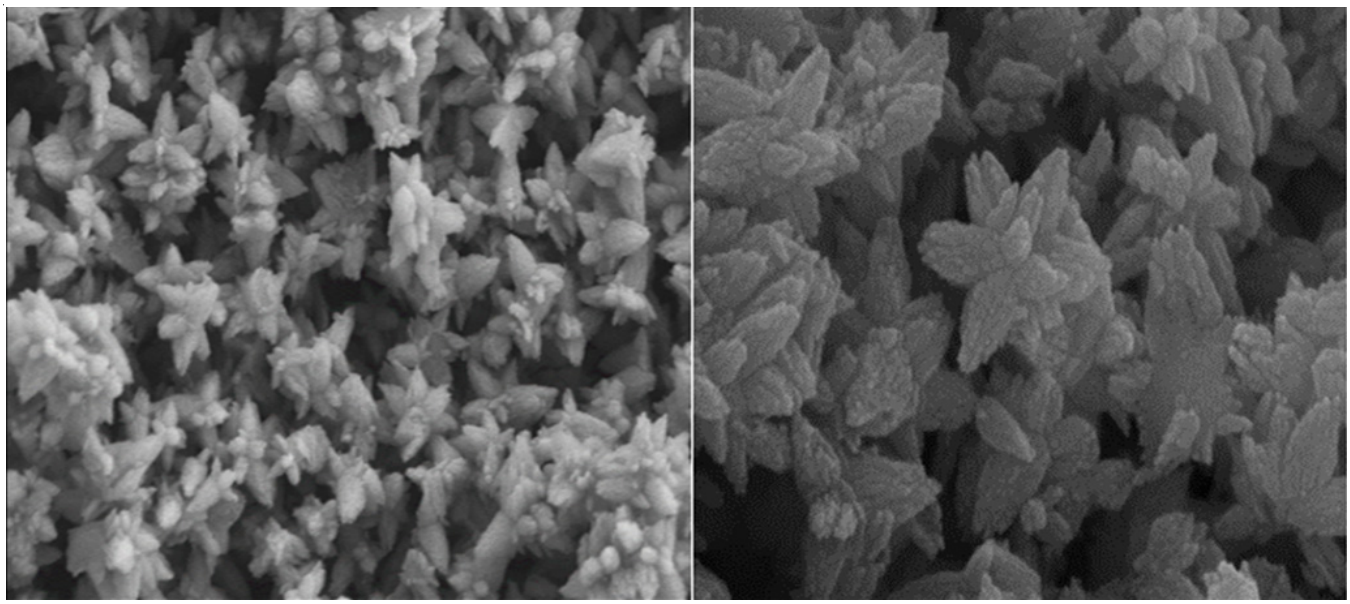

Fig. 5. SEM images of *Rivea hypocrateriformis* mediated ZnO nanoparticles

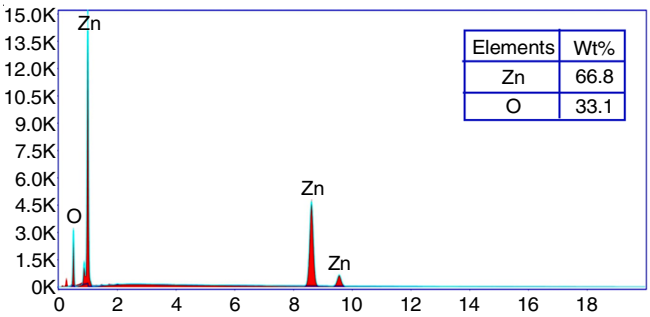


Fig. 6. EDS image of *R. hypocrateriformis* mediated ZnO nanoparticles

**Antioxidant activity:** It was found that the OH-DPPH solution was transformed into the non-radical form of DPPH-H, resulting in the scavenging of DPPH, by removing an electron or hydrogen atom from an antioxidant component, specifically RH-ZnO NPs [13]. The optical absorbance at 517 nm changes demonstrated quantitative decolorization of DPPH with electron transfer from the antioxidant RH-ZnO NPs. Table-1 displays the results of the DPPH assay, which used ascorbic acid, to measure the antioxidant activity of the synthesized RH-ZnO NPs. The RH-ZnO NPs demonstrated scavenging activities

TABLE-1
ANTIOXIDANT ACTIVITY OF
RH-ZnO NPs BY DPPH ASSAY METHOD

| RH-ZnONPs concentration (µg/mL) | Percentage of inhibition in triplicates | | | Mean value (%) |
|---|---|---|---|---|
| Ascorbic acid | 97.70313 | 96.8418 | 96.55469 | 97.03321 |
| 500 | 89.03244 | 89.49182 | 90.69767 | 89.74065 |
| 250 | 74.07407 | 73.90181 | 87.71174 | 78.56254 |
| 100 | 47.94717 | 66.37956 | 66.46569 | 60.26414 |
| 50 | 30.14643 | 19.17887 | 16.82458 | 22.04996 |
| 10 | 1.234568 | 0.574218 | 13.66638 | 5.158388 |

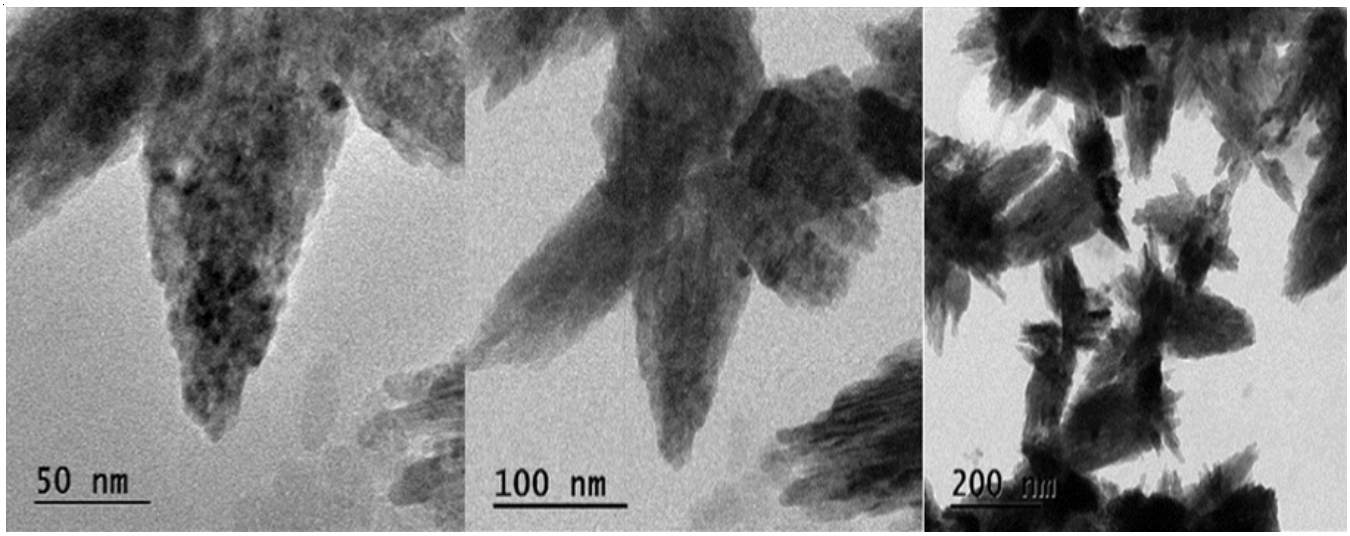


Fig. 7. TEM images of *Rivea hypocrateriformis* mediated ZnO nanoparticles

of 89.74% at their maximum concentration (500 µg/mL), when compared to conventional ascorbic acid in terms of absorbance. According to the findings, RH-ZnO NPs exhibit antioxidant capabilities that are on equivalent with ascorbic acid (97.03%). It was also observed that the antioxidant activity of the synthesized nanoparticles increased with increasing concentration.

**Anticancer activity:** The *in vitro* anticancer activity of the synthesized RH-ZnO NPs at different concentrations ranging from 1-500 µg/mL was assessed using the MTT assay. The sample exhibited minimum effect against normal cell lines which confirmed the specific effect of the synthesized RH-ZnO NPs on the cancer cells. The anticancer activity increase with increasing the RH-ZnO NPs concentration. The size and dosage play a major in inducing toxicity [14]. From Table-2, it was found that ZnO nanoparticles synthesized from the *R. hypocrateriformis* extract showed excellent activity on cancer cell lines. These nanoparticles exhibited potent activity against A549 cell line with $IC_{50}$ value 59.75 µg/mL.

The alternation in the morphology of A549 cell line and synthesized RH-ZnO NPs at various concentration (500, 300, 100, 50, 25 and 1 µg/mL) are shown in Fig. 8. It could be observed that control cell did not show any significant changes on their morphology. Nevertheless, when nanoparticles are present, there is an enhancement in cell distortion, membrane blebbing and the movement of cells in a concentration dependent manner.

TABLE-2
ANTICANCER ACTIVITY OF RH-ZnO NANOPARTICLES CELL VIABILITY (%)

| RH-ZnONPs concentration (µg/mL) | Cell viability (%) (in triplicates) | | | Mean value (%) |
|---|---|---|---|---|
| Control | 100 | 100 | 100 | 100 |
| 500 | 56.3969 | 62.0513 | 57.0648 | 58.504314 |
| 400 | 66.4926 | 67.6923 | 62.0609 | 65.415267 |
| 300 | 69.7998 | 69.8291 | 63.7783 | 67.802395 |
| 200 | 71.9756 | 70.7692 | 67.2131 | 69.985992 |
| 100 | 75.1088 | 74.1026 | 67.6815 | 72.297618 |
| 50 | 75.9791 | 77.5214 | 72.0531 | 75.184521 |
| 25 | 86.5970 | 85.3846 | 79.6253 | 83.868983 |
| 10 | 89.8172 | 91.4530 | 83.8407 | 88.370324 |
| 5 | 95.0392 | 94.7009 | 86.8852 | 92.208422 |
| 1 | 97.2150 | 96.4957 | 89.6956 | 94.468749 |

**Acridine orange/ethidium bromide staining:** The apoptosis induction was evaluated using fluorescence microscopy after staining with acridine orange/ethidium bromide (AO/EtBr), following treatment with the $IC_{50}$ concentration of RH-

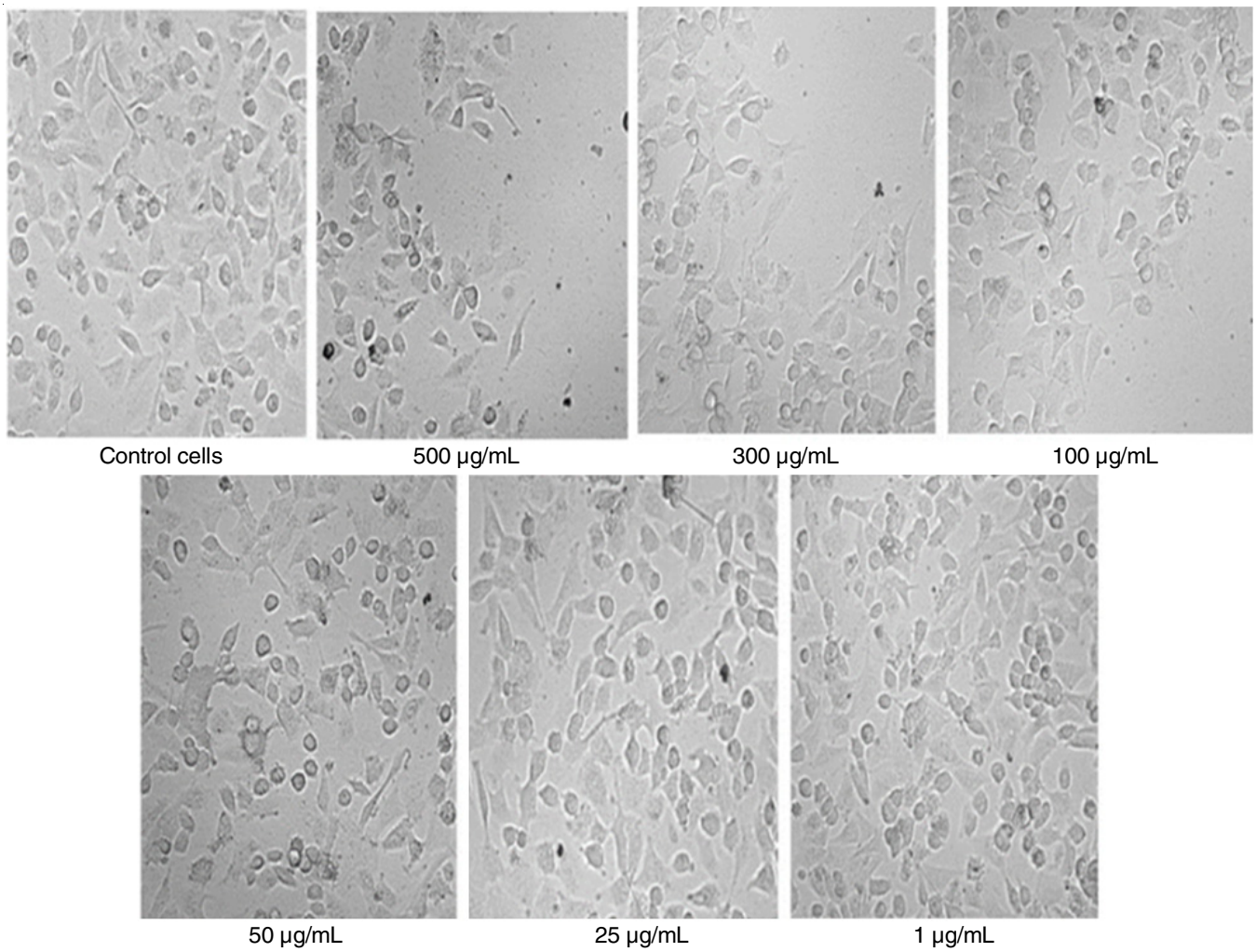


Fig. 8. Morphological changes in control and RH-ZnO NPs treated Lung cancer A549 cells for 24 h

ZnO NPs and the results are shown in Fig. 9. Acridine orange is able to enter normal cell membranes, causing the cells to emit green fluorescence. However, in apoptotic cells and apoptotic bodies resulting from nuclear shrinkage and damage, orange-colored bodies are observed. Necrotic cells, on the other hand, emit red fluorescence due to their loss of membrane integrity when observed under a fluorescence microscope.

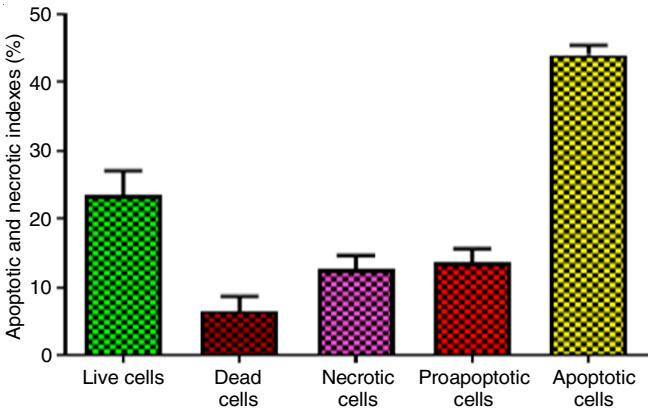


Fig. 9. Apoptotic and necrotic indexes %

## Conclusion

The present investigation has proven that the successful synthesis of ZnO nanoparticles from *Rivea hypocrateriformis* plant extract using green synthetic method. The UV-visible spectrum confirmed the absorbance peak between 287 nm, whereas the XRD patterns showed the flower shaped (hexagonal) phase of synthesized ZnO nanoparticles. The ZnO nanoparticles exhibit good stability because of the repulsion between the particles, which is ensured by the negative sign of the zeta potential value. The SEM confirmed the shape and size of the synthesized nanoparticles, whereas the TEM images justified the inner micrography of SEM which showed flower shape. The *in vitro* antioxidant assays carried out showed good activity of RH-ZnO NPs synthesized through green method. Moreover, the synthesized nanoparticles also showed a considerable cytotoxicity against the A549 cancer cell lines without affecting the normal cells.

## CONFLICT OF INTEREST

The authors declare that there is no conflict of interests regarding the publication of this article.

## REFERENCES

1. F. Mottaghitalab, M. Farokhi, Y. Fatahi, F. Atyabi and R. Dinarvand, *J. Control. Release*, **295**, 250 (2019); https://doi.org/10.1016/j.jconrel.2019.01.009
2. A.C. MacKinnon, J. Kopatz and T. Sethi, *Br. Med. Bull.*, **95**, 47 (2010); https://doi.org/10.1093/bmb/ldq023
3. O. Oyebode, N.-B. Kandala, P.J. Chilton and R.J. Lilford, *Health Policy Plan*, **31**, 984 (2016); https://doi.org/10.1093/heapol/czw022
4. S.S. Saboo, S. Khadabadi and G.G. Tapadiya, *Asian Pac. J. Trop. Dis.*, **2(Suppl.1)**, S503 (2012); https://doi.org/10.1016/S2222-1808(12)60211-4
5. N. Krithiga, A. Rajalakshmi and A. Jayachitra, *J. Nanosci.*, **2015**, 928204 (2015); https://doi.org/10.1155/2015/928204
6. Ü. Özgür, Y.I. Alivov, C. Liu, A. Teke, M.A. Reshchikov, S. Doğan, V. Avrutin, S.-J. Cho and H. Morkoç, *J. Appl. Phys.*, **98**, 041301 (2005); https://doi.org/10.1063/1.1992666
7. R. Resmi, J. Yoonus and B. Beena, *Mater. Today Proc.*, **46**, 3062 (2021); https://doi.org/10.1016/j.matpr.2021.02.498
8. R. Dobrucka and J. Dlugaszewska, *Saudi J. Biol. Sci.*, **23**, 517 (2016); https://doi.org/10.1016/j.sjbs.2015.05.016
9. R. Yuvakkumar, J. Suresh, B. Saravanakumar, A.J. Nathanael, S.I. Hong and V. Rajendran, *Spectrochim. Acta A Mol. Biomol. Spectrosc.*, **137**, 250 (2015); https://doi.org/10.1016/j.saa.2014.08.022
10. R.Y. Hong, J.H. Li, L.L. Chen, D.Q. Liu, H.Z. Li, Y. Zheng and J. Ding, *Powder Technol.*, **189**, 426 (2009); https://doi.org/10.1016/j.powtec.2008.07.004
11. K.M. Kumar, B.K. Mandal, E.A. Naidu, M. Sinha, K. Siva Kumar and P.S. Reddy, *Spectrochim. Acta A Mol. Biomol. Spectrosc.*, **104**, 171 (2013); https://doi.org/10.1016/j.saa.2012.11.025
12. J. Fowsiya, G. Madhumitha, N.A. Al-Dhabi and M.V. Arasu, *J. Photochem. Photobiol. B*, **162**, 395 (2016); https://doi.org/10.1016/j.jphotobiol.2016.07.011
13. M. Hosny and M. Fawzy, *Adv. Powder Technol.*, **32**, 2891 (2021); https://doi.org/10.1016/j.apt.2021.06.004
14. F.S. Freyria, B. Bonelli, M. Tomatis, M. Ghiazza, E. Gazzano, D. Ghigo, E. Garrone and B. Fubini, *Chem. Res. Toxicol.*, **25**, 850 (2012); https://doi.org/10.1021/tx2004294